Aus dem Universitätsklinikum Münster

Klinik für Kinder- und Jugendmedizin - Allgemeine Pädiatrie

Direktor: Univ.-Prof. Dr. med. Heymut Omran

Molecular characterization of IDA defects caused by mutations in genes encoding for the 96 nm axonemal ruler proteins CCDC39 and CCDC40 in human respiratory cilia

INAUGURAL – DISSERTATION

zur

Erlangung des doctor medicinae

der medizinischen Fakultät

der Westfälischen Wilhelms-Universität Münster

vorgelegt von Wolter, Alexander

aus Hagen

2020

Dekan: Univ.-Prof. Dr. med. Frank U. Müller

1. Berichterstatter: Direktor: Univ.-Prof. Dr. med. Heymut Omran
2. Berichterstatter: Univ.-Prof. Dr. med. Rainer Wiewrodt
Tag der mündlichen Prüfung: 20.01.2020

Aus dem Universitätsklinikum Münster
Klinik für Kinder- und Jugendmedizin - Allgemeine Pädiatrie
Direktor: Univ.-Prof. Dr. med. Heymut Omran
Referent: Univ.-Prof. Dr. med. Heymut Omran
Koreferent: Univ.-Prof. Dr. med. Rainer Wiewrodt

ZUSAMMENFASSUNG

Molecular characterization of IDA defects caused by mutations in genes encoding for the 96 nm
axonemal ruler proteins CCDC39 and CCDC40 in human respiratory cilia
Wolter, Alexander

Die Primäre ziliäre Dyskinesie (PCD) wird durch Mutationen in Genen verursacht, welche für die Struktur und die Assemblierung des Ziliums von Bedeutung sind. Mutationen in *CCDC39* und *CCDC40* verursachen Defekte in dem sogenannten „96 nm axonemal ruler" (zu dt. axonemales Lineal), welches für die 96 nm Periodizität aller axonemalen Strukturen, wie z.B. der inneren Dyneinarme (IDAs) in eukaryotischen Zilien und Flagellen, verantwortlich ist. Dieser Proteinkomplex, bestehend aus CCDC39 und CCDC40, reguliert die Verankerung der Radialspeichen, des Nexin-Dynein-regulatory-complexes (N-DRC) als auch der IDAs [40]. Die Gruppe der IDAs lässt sich in einen doppelköpfigen Dyneinarm I1 sowie sechs einköpfige Dyneinarme unterteilen, welche wiederum je nach ihrer Assoziation mit DNALI1 oder Centrin den Gruppen I2 und I3 zugeordnet werden.

Mittels Immunfluoreszenzmikroskopie mit Antikörpern gegen einen Bestandteil des N-DRCs (GAS8) und gegen DNALI1 wurde bisher gezeigt, dass Mutationen in *CCDC39* und *CCDC40* zum Verlust des N-DRCs und der IDAs der Gruppe I2 führen [4, 36]. Durch Immunfluoreszenzfärbungen mit je einem Antikörper gegen DNAH1, DNAH6 und DNAH7 konnte ich in meiner Arbeit zeigen, dass Mutationen in *CCDC39* und *CCDC40* zu einem Defekt der IDAs der Gruppe I2 *sowie* der Gruppe I3 führen. Indem ich die Abwesenheit von DNAH1 in humanen Zilien mit diesen Mutationen nachgewiesen habe, bestätigte ich die Abwesenheit der IDAs der Gruppe I2, die bisher nur durch Abwesenheit von DNALI1 gezeigt werden konnte. In Zukunft kann der Anti-DNAH1-Antikörper daher in der PCD-Diagnostik eingesetzt werden, um das Fehlen der IDAs der Gruppe I2 zu bestätigen. Mittels Immunfluoreszenzmikroskopie mit Antikörpern gegen DNAH6 und DNAH7 konnte ich auch erstmalig zeigen, dass Mutationen in *CCDC39* und *CCDC40* ebenfalls zur Abwesenheit der IDAs der Gruppe I3 führen. Es ist das erste Mal, dass auch IDAs der Gruppe I3 und damit beide Gruppen der einköpfigen IDAs (I2 und I3) in humanen Zilien systematisch analysiert wurden. Mit diesen drei Antikörpern stehen nun wertvolle Werkzeuge zur Verfügung, um die Zusammensetzung der IDAs zu charakterisieren und die PCD Diagnostik zu verbessern.

Tag der mündlichen Prüfung: 20.01.2020

Erklärung

Ich gebe hiermit die Erklärung ab, dass ich die Dissertation mit dem Titel:

„Molecular characterization of IDA defects caused by mutations in genes encoding for the 96 nm axonemal ruler proteins CCDC39 and CCDC40 in human respiratory cilia "

Klinik für Kinder- und Jugendmedizin - Allgemeine Pädiatrie

unter der Anleitung von Univ.-Prof. Dr. med. Heymut Omran

1. selbstständig angefertigt,
2. nur unter Benutzung der im Literaturverzeichnis angegebenen Arbeiten angefertigt und sonst kein anderes gedrucktes oder ungedrucktes Material verwendet,
3. keine unerlaubte fremde Hilfe in Anspruch genommen,
4. sie weder in der gegenwärtigen noch in einer anderen Fassung einer in- oder ausländischen Fakultät als Dissertation, Semesterarbeit, Prüfungsarbeit, oder zur Erlangung eines akademischen Grades, vorgelegt habe.

Ort, Datum: Münster, den 11.07.2018   Name: Alexander Wolter

Unterschrift:

Table of Contents

List of abbreviations

Table 1: List of abbreviations

Abbreviation	Explanation
µl	Microliter
µm	Micrometer
ARMC4	Armadillo Repeat Containing Protein 4
C21ORF59	Chromosome 21 Open Reading Frame 59
CCDC114	Coiled-Coil Domain-Containing Protein 114
CCDC151	Coiled-Coil Domain-Containing Protein 151
CCDC164	Coiled-Coil Domain-Containing Protein 164
CCDC39	Coiled-Coil Domain-Containing Protein 39
CCDC40	Coiled-Coil Domain-Containing Protein 40
CCDC65	Coiled-Coil Domain-Containing Protein 65
CP	Central pair
DHC 1	Dynein Heavy Chain 1
DHC 2	Dynein Heavy Chain 2
DHC 5	Dynein Heavy Chain 5
DHC 6	Dynein Heavy Chain 6
DHC 7	Dynein Heavy Chain 7
DHC 8	Dynein Heavy Chain 8
DHC 9	Dynein Heavy Chain 9
DHC 10	Dynein Heavy Chain 10
DIC	Differential interference contrast microscopy images
DNAAF1/LRRC50	Dynein Axonemal Assembly Factor 1 (=LRRC50)
DNAAF2/KTU	Dynein Axonemal Assembly Factor 2 (= KTU)
DNAAF3/PF22	Dynein Axonemal Assembly Factor 3
DNAH1	Dynein Axonemal Heavy Chain 1
DNAH5	Dynein Axonemal Heavy Chain 5
DNAH6	Dynein Axonemal Heavy Chain 6
DNAH7	Dynein Axonemal Heavy Chain 7
DNAH11	Dynein Axonemal Heavy Chain 11
DNAI1	Dynein Axonemal Intermediate Chain 1
DNAI2	Dynein Axonemal Intermediate Chain 2
DNAL1	Dynein Axonemal Light Chain 1
DNALI1	Dynein Axonemal Light Intermediate Chain 1
Dynein a	IDA group I2, dynein a
Dynein b	IDA group I3, dynein b
Dynein c	IDA group I2, dynein c
Dynein d	IDA group I2, dynein d
Dynein e	IDA group I3, dynein e
Dynein f	IDA group I1, dynein f
Dynein g	IDA group I3, dynein g
DYX1C1/DNAAF4	Dyslexia Susceptibility 1 Candidate 1 (= DNAAF4)
f/I1	IDA group I1, dynein f
FAP120	Flagellar Associated Protein
g	Gram
GAS8	Growth Arrest-Specific 8
HC	Heavy Chain
HEATR2/DNAAF5	HEAT-Repeat Containing Protein 2
HVMA	High-speed video microscopy analysis
IC138	Flagellar inner arm intermediate chain IC138
IC140	Flagellar inner arm intermediate chain IC140
IC97	Flagellar inner arm intermediate chain IC97
ICLC	Intermediate chain and light chain complex
IDA	Inner dynein arm
IF	High resolution immunofluorescence
IFT	Intraflagellar transport
kDa	Kilodalton
KTU	Kintoun (= DNAAF2)

LC7a	Flagellar outer dynein arm light chain LC7
LC7b	Roadblock/lc7 family protein
LC8	Outer dynein arm light chain 8
LRRC6	Leucine Rich Repeat Containing Protein 6
LRRC50	Leucine Rich Repeat Containing Protein 50 (= DNAAF1)
mg	Milligram
min	Minutes
ml	Milliliters
mm	Millimeters
MTDs	Microtubule doublets
NaOH	Sodium hydroxide
N-DRC	Nexin-dynein-regulatory complex
nm	Nanometers
o/n	Over night
ODA	Outer dynein arm
ODA-DC	ODA docking complex
p28	28-kDa protein, IDA component in *C. reinhardtii*
PBS	Phosphate buffered saline
PCD	Primary ciliary dyskinesia
pf-7	Paralyzed flagella 7
pf-8	Paralyzed flagella 8
PFA	Paraformaldehyde
PIH1D3	Protein Interacting with HSP90Domain Containing Protein 3
RPMI	Roswell Park Memorial Institute medium
RS	Radial spokes
RSPH4A	Radial spoke head 4A
RSPH9	Radial spoke head 9
RT	Room temperature
SPAG1	Sperm associated antigen 1
Tctex1	T-Complex-Associated-Testis- Expressed 1
Tctex2b	T-Complex-Associated-Testis- Expressed 2b
TEM	Transmission electron microscopy
TTC25	Tetratricopeptide repeat domain containing protein 25
TXNDC3	Thioredoxin Domain-Containing Protein 3
ZMYND10	Zinc Finger MYND-Type Containing Protein 10

1 Introduction

Cilia and flagella are related organelles with structures that are highly conserved across 1.6 billion years [49].

They have a specific ultrastructure, comprising nine peripheral microtubule doublets (MTDs) around one central pair (CP) (Figure 1). Furthermore, they contain several force generating inner (IDAs) and outer dynein arms (ODAs). Radial spoke complexes (RSs) connect the CP with the outer doublets in order to provide signal transduction between the center and the dynein arms to coordinate ciliary beat and waveform [3]. Whereas the nexin-dynein regulatory complex (N-DRC) plays an important role in inner dynein arm attachment and regulation [20]. Ciliated cells in humans can also lack the central pair. Consequently they appear in four different forms, depending on the motility and the availability of a central pair: 9+2 motile cilia (respiratory epithelium, ependymal cells, fallopian tube and sperm flagella), 9+2 immotile cilia (kinocilia of hair-cells = stereocilia), 9+0 motile cilia (nodal cilia) and 9+0 immotile cilia (renal monocilia, photoreceptor-connecting cilia, bile duct, pancreatic duct, bone and cartilage) [3, 15].

Primary ciliary dyskinesia (PCD) is a genetically heterogeneous disorder, which is caused by defects in the morphology and motility of cilia and sperm flagella. PCD individuals suffer from recurrent respiratory tract infections due to disturbed or absent mucociliary clearance. Bronchiectasis, otitis media, chronic sinusitis and subfertility are often observed as a consequence of PCD. The body's left-right-asymmetry, which is determined by nodal cilia in the ventral node during embryogenesis, can be affected too. Almost half of the PCD individuals have *situs inversus totalis*. PCD together with *situs inversus totalis* is known as "Kartagener syndrome" [1].
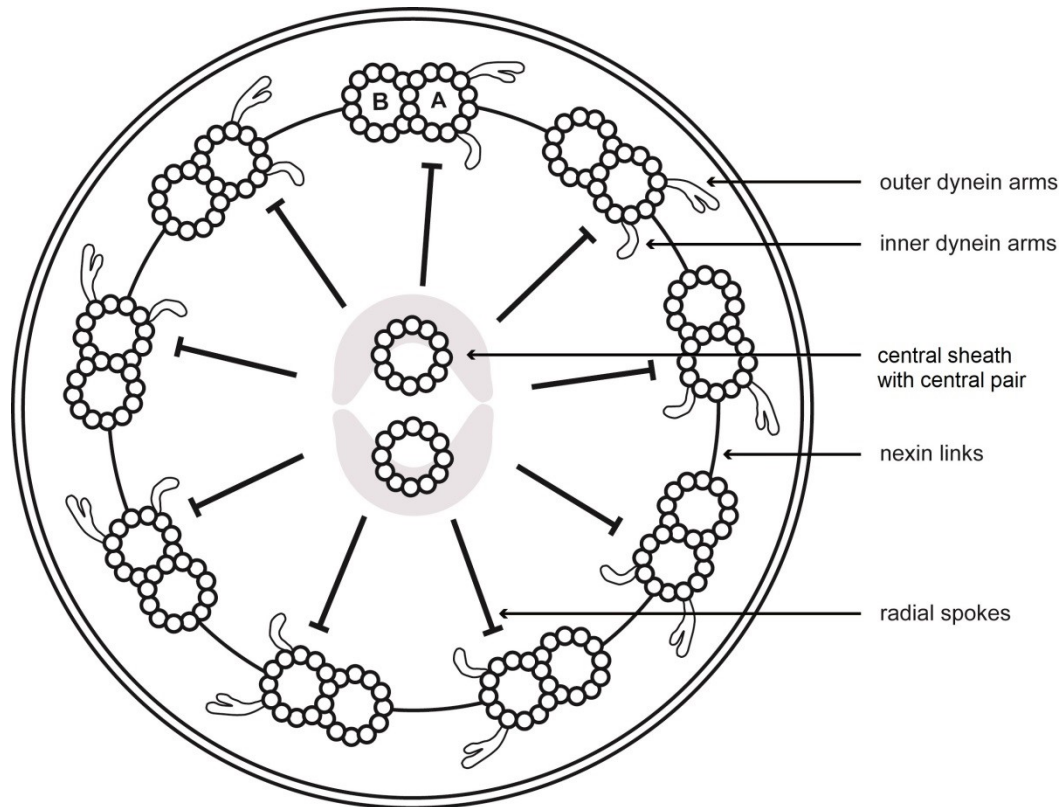
Introduction

Figure 1: Cross section of a 9+2 cilium

A 9+2-motile-cilium comprises nine outer microtubule doublets (A and B-tubules) around one central pair, which itself is surrounded by a central sheath. Radial spokes connect the central pair with the peripheral doublets and provide signal transduction between these two parts. The outer doublets are joined via nexin-links. Inner and outer dynein arms are attached to the A-tubule. Figure adapted from [63].

PCD is caused by a variation of mutations in genes encoding proteins important for the ultrastructure and assembly of motile cilia. Most PCD cases are due to ODA or ODA-docking (ODA-DC) defects (*DNAH5, DNAI1, DNAI2, DNAL1, TXNDC3 and CCDC114, CCDC151, ARMC4, TTC25*) [2, 14, 21, 27, 33, 35, 41, 45, 46, 50, 62].

Defects of the radial spoke head (i.e. mutations in *RSPH4A* and *RSPH9*) result in absence of the central pair and transposition of MTDs [8]. However, CP and RS defects are difficult to discern by transmission electron microscopy (TEM). Whereas loss of function of proteins involved in the cytoplasmic preassembly of dynein arms (DNAAF1/LRRC50, DNAAF2/KTU, DNAAF3/PF22, DYX1C1/DNAAF4, HEATR2/DNAAF5, LRRC6, SPAG1, C21ORF59, ZMYND10, PIH1D3) causes combined defects of IDAs and ODAs [13, 22, 30,

32, 37, 43, 47]. Mutations can also affect the central pair (*HYDIN*) or *DNAH11*, which causes PCD without ultrastructural alterations observed by TEM [2, 28, 42].

Mutations in *CCDC39* [36] and *CCDC40* [4] result in defects of the 96 nm axonemal ruler [40]. *CCDC39* and *CCDC40* encode related proteins that are localized to the axoneme and contain coiled-coil domains [3, 4, 36]. Oda et al. recently showed that pf-8 and pf-7, the *Chlamydomonas* orthologues of CCDC39/40, are functioning as a 96 nm axonemal ruler, which determines the repeat length in eukaryotic cilia and flagella (Figure 2). They have shown that pf-7 and pf-8 form a complex that is responsible for the 96 nm periodicity in MTDs. It is likely that the pf-7/8-complex regulates anchoring of IDAs and the N-DRC providing anchoring sites for these protein complexes [40].
Mutations in *CCDC39* and *CCDC40* affect at least 12% of all PCD cases [9, 48, 58]. The phenotype is characterized by disorganization of the 9+2 microtubule arrangement observed by TEM [1]. The nine peripheral microtubules are not altered in their number, but they are often mislocalized. Whereas the central pair is either missing (9+0), mislocalized (9+2) or increased in number (9+4) [1, 1]. Furthermore, defects of the 96 nm axonemal ruler result in mislocalization or absence of IDAs [1, 4, 36] and the N-DRC [4, 29, 36, 57]. Finally, 30% of all ciliated cells with mutations in *CCDC39* and *CCDC40* are completely immotile. The motility of the other 70% is reduced in amplitude and shows a lower beat frequency with stiff beating pattern [4, 9, 36]. Davis et al. evaluated clinical features of PCD in childhood and came to the conclusion that children with biallelic mutations in *CCDC39* and *CCDC40* or associated ultrastructural defects have worse lung disease and poorer growth compared to those with ODA defects [10].

By using antibodies directed against DNALI1 and GAS8 it was shown that IDAs and the N-DRC are absent from the ciliary axoneme of PCD individuals with mutations in *CCDC39* and *CCDC40* [4, 36].

In *Chlamydomonas* seven inner dynein arm isoforms have been reported with at least eight different heavy chains. One double-headed inner dynein arm f/I1,

which contains two dynein heavy chains (DHC1 and DHC10). The remaining six single-headed inner dynein arms (a, b, c, d, e, and g) each carries distinct dynein heavy chains (DHC6, DHC5, DHC9, DHC2, DHC8 and DHC7) [25, 56]. The IDAs are arranged in a 96 nm-repeat along the entire axoneme and show a specific order (Figure 2). Nevertheless, this is true for seven of nine microtubule doublets with two of them showing a different structure in *Chlamydomonas reinhardtii* [7].
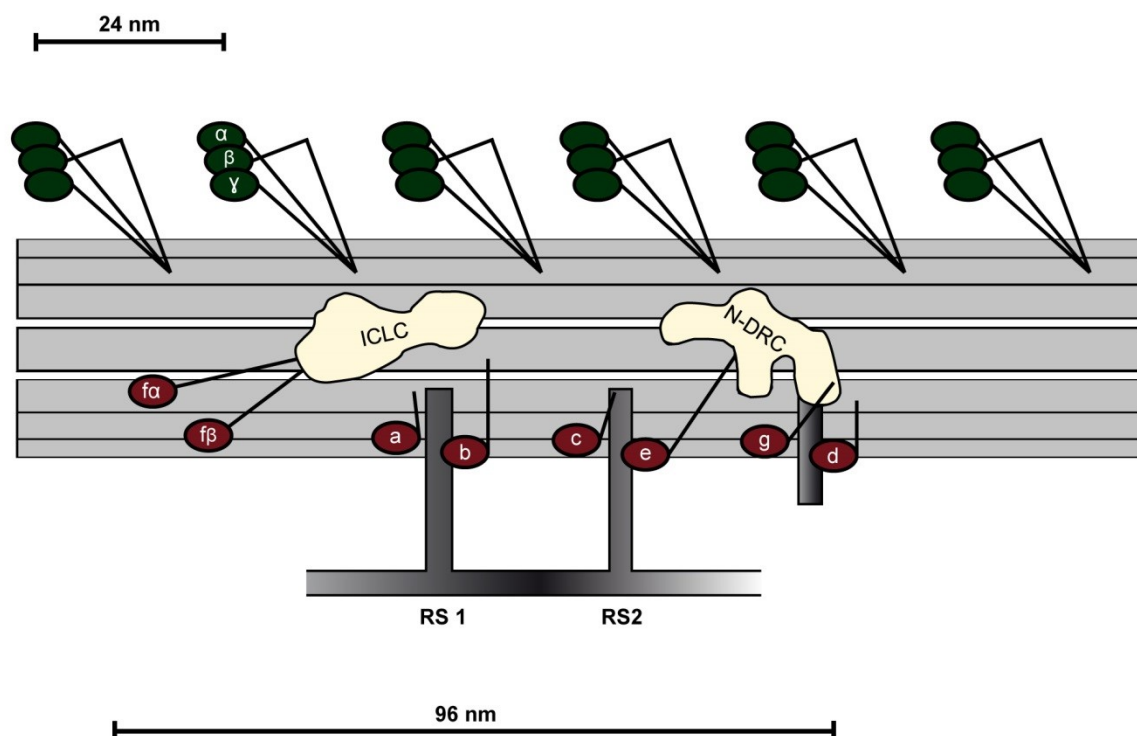

Figure 2: Arrangement of inner dynein arms in the axoneme of *Chlamydomonas reinhardtii*

Seven out of nine outer microtubule doublets show a specific arrangement of inner dynein arms, which is repeated every 96 nm. The outer dynein arms comprise three heavy chains and form however a unit which is repeated every 24 nanometers. Based on the number of heavy chains, inner dynein arms are divided into two groups. One double-headed f/I1, comprising two dynein heavy chains and six single-headed dynein isoforms with just one dynein heavy chain. Bui et al. took also the position of the single-headed dyneins towards the radial spokes into consideration. Dyad1 (a and b) is located proximally and distally to radial spoke 1. Dyad2 (c and e) is located proximally and distally to RS2 and dyad3 (g and d) is located distally to RS2. Isoform f/I1 however, is located in the outer periphery of the 96 nm repeat. Figure adapted from [7].

The double-headed isoform has a rather complex subunit composition with two heavy chains (α and β) and the I1 intermediate chain and light chain complex

Introduction

(ICLC), which itself consists of three intermediate chains (IC97, IC138 and IC140) and five light chains (LC8, LC7a, LC7b, Tctex1 and Tctex2b) as well as the associated protein FAP120 (Table 2) [11, 12, 16–19, 23, 34, 38, 39, 51, 52, 54, 55, 59, 64]. Heuser et al. recently described a possible composition and architecture of the double-headed isoform f/I1 (Figure 3) using 3D cryoelectron tomography microscopy. They showed that the IDA isoform f/I1 is localized between RS1 and the ODA row and defined seven distinct connections to its surroundings. It is therefore likely that f/I1 plays an important role as a regulatory complex [19]. Reduced motility has been observed in flagella of *Trypanosoma brucei* and *Chlamydomonas reinhardtii* with defects in IDA isoform f/I1 [39, 60]. The I1α dynein heavy chain (HC) is connected to the A-tubulus and gives therefore rise to the assumption that it takes a regulating function. I1β-HC however is supposed to generate the force [19, 39, 51, 52, 61].
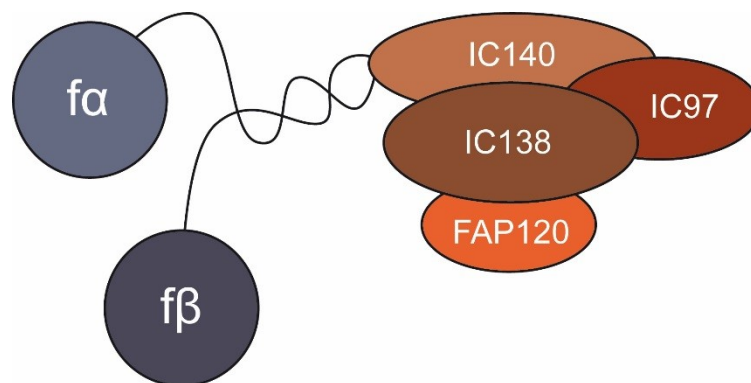

Figure 3: Double-headed inner dynein arm isoform f/I1 in *Chlamydomonas reinhardtii*

The subunit composition of IDA group I1 is very complex. It consists of two dynein heavy chains (α- and β-heavy chain) and the ICLC (intermediate chain and light chain complex). The ICLC comprises three intermediate chains (IC140, IC138, IC97) and five light chains (LC8, LC7a, LC7b, Tctex1 and Tctex2b), which are not shown in this figure. Furthermore, the protein FAP120 is associated with one of the intermediate chains. Both heavy chains are connected to the ICLC via IC140. Figure adapted from [19].

In contrast to the double-headed isoform f/I1, single-headed inner dynein arms are all associated with the intermediate chain actin and either the light chain p28 or centrin (Table 2) [31, 53, 66]. Based on these findings the single-headed dyneins are further classified into the p28-associated subgroup I2 (a, c and d)

and the centrin-associated subgroup I3 (b, e and g) (Figure 4). Another classification takes the position of the different IDAs towards the RSs into consideration. Dyad1 (dyneins a and b) is located proximally and distally to the RS1, dyad2 (dyneins c and e) is located in the same manner to RS2 and finally dyad3 (dyneins d and g) is located distally to RS2 (Figure 2) [6, 7].
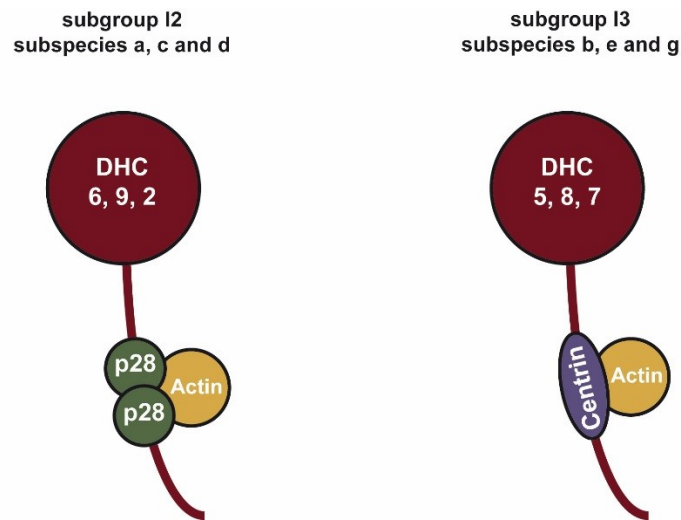

Figure 4: Single-headed inner dynein arm isoforms of subgroup I2 and I3 in *Chlamydomonas reinhardtii*

Inner dynein arm subspecies a, c and d belong to subgroup I2. They comprise their appropriate dynein heavy chain, which is attached to actin and two light chains p28, which is the orthologue to the human light chain DNALI1. Inner dynein arm subspecies b, e and g however form subgroup I3. They also contain their appropriate dynein heavy chain, which is attached to actin. In contrast to I2 the dyneins of subgroup I3 are associated with centrin instead of p28. Figure adapted from [66].

The diagnosis of IDA-defects is very complex. IDA-components show less contrast in TEM and are therefore difficult to detect. Due to the relatively long 96 nm-repeating pattern of each IDA (ODAs are arranged in a 24 nm periodicity), IDAs appear in smaller amounts than ODAs in cross sections. This makes IDA alterations more difficult to analyze and leads to the assumption that many PCD individuals with altered IDA-components are falsely diagnosed or even remain undiagnosed.

Isolated IDA defects are relatively rare and have just been reported for DNAH1 [5, 24]. So far, defects of the IDAs were shown only in combination with ODA

defects caused by mutations in genes encoding cytoplasmic preassembly factors or in combination with defects of the N-DRC caused by defects of the 96 nm axonemal ruler [3].

The aim of my work was to specify which and to what extent IDAs are affected by defects of the 96 nm axonemal ruler. To accomplish this I used high-resolution immunofluorescence (IF) microscopy and specific antibodies directed against components of the IDA subgroup I2 (DNAH1) and IDA subgroup I3 (DNAH6 and DNAH7) (Table 2) to describe the IDA defects caused by mutations in genes encoding the 96 nm axonemal ruler proteins CCDC39 and CCDC40. Prior to my work the mentioned antibodies were established by Inga M. Höben as documented in her master´s thesis: "Molecular Mechanisms Involved in Primary Ciliary Dyskinesia with Outer and Inner Dynein Arm Defects".

Table 2: Inner dynein arm components in *Chlamydomonas reinhardtii* and their human orthologues

The IDAs in *Chlamydomonas reinhardtii* are divided into one double-headed isoform f of group I1 and six single-headed isoforms (a, b, c, d, e, g and minor dyneins). The double-headed f/I1 comprises the α- and β-heavy chain as well as the ICLC (intermediate chain and light chain complex), which itself consists of three intermediate chains and five light chains. The single-headed isoforms are all associated with actin as their intermediate chain. Single-headed dyneins of subgroup I2 are associated with p28 (a, c, d), which is the orthologue to the human light chain DNALI1. The single-headed dyneins of subgroup I3 are associated with centrin instead of p28 (b, e, g). Minor dyneins can replace certain major dyneins in the proximal axoneme [6, 65]. The last row shows some of the human orthologous heavy chains. Table adapted from King and Kamiya 2009 [26] and Yagi et al. 2009 [65].

Type	double-headed	single-headed									
Subspecies	f/I1	a	b	c	d	e	g	minor dyneins			
DHC	1, 10	6	5	9	2	8	7	3	4	11	12
IC/LC — IC140											
IC138											
IC97											
					p44						
		actin	actin	actin	actin	actin	actin	actin	actin	actin	actin
					p38						
		p28		p28	p28						
			centrin			centrin	centrin	centrin	centrin		
Tctex1											
Tctec2b											
LC7a, b											
LC8											

Human orthologue	DNAH10		DNAH7		DNAH1		DNAH6	DNAH6			

2 Materials and Methods

2.1 Methods

2.1.1 PCD Individuals

This study was approved by the ethics committee of the University Children's Hospital Muenster- Department of General Pediatrics. All candidates gave written informed consent. Transnasal brush biopsies and blood samples were collected from a large cohort of PCD individuals showing the recruitment criteria of PCD. Most PCD individuals included in this study carry either mutations in *CCDC39* or *CCDC40* (Table 3 and Table 4). Four PCD individuals carry either mutations in *GAS8*, *CCDC164*, *CCDC65* or *DNAH5* (Table 12).

Table 3: Summary of IF-results for PCD individuals (PCD ind.) with mutations in *CCDC39*

PCD ind.	Mutation in *CCDC39*	DNAH1	DNAH6	DNAH7
OP-122	[p.Thr358Glnfs*3]+[p.Lys336Argfs*19]	-	-	-
OP-336 II1	ex. 9: c.1036-2A>C hom.	-	-	-
OP-632 II1	ex.17:c.2346_2351delTTTCA het.	-	-	-
OI-5 II1	[p.Glu471*]+[p.Glu471*]	-		-
OP-736	[p.Glu851*]+splicing-mut.	-		-
OP-737; (related to OP-736)	[p.Glu851*]+splicing-mut.	-		-
OP-777	c.610-2A>G het.	?		-
OP-868	c.2596G>T, p.Glu866* hom.	-		-

Table 4: Summary of IF-Results for PCD individuals with mutations in *CCDC40*

PCD ind.	Mutation in *CCDC40*	DNAH1	DNAH6	DNAH7
F-727 II1	[p.Ala83Valfs82*]+[p.Ala83Valfs82*]	-		-
F-677II1 (OP73W)	[p.Ala83Valfs82*]+n.d.	-	-	-
OP-57 II	[p.Gln651*] +[p.Gln651*]	-		-
OP-76 II1	Asp1044Serfs35*]+[p.Asp1044Ser fs35*]	-	-	-
OP-82 II1	[p.Ala83Valfs82*]+[p.Gln604*]	-?		-
OP-87 II2	[p.Ala83Valfs82*]+[p.Glu260Argfs25*]	-		-
OP-120	p.Ala83Valfs82*]+[p.Ala83Valfs82*]	-		
OP-277 II1	[p.Arg942MetinsTrp]+[p.Gln1043 fs36*]	-	-	-
OP-659	[p.Arg321*]+[p.Arg814*]	-		-
OI-101 II1	del ex 4-7 hom.	-	-	-
OP-712 II1	[p.Asp510Serfs22*]+[p.Asp510Ser fs22*]	-		
OP-712 II2	[p.Asp510Serfs22*]+[p.Asp510Ser fs22*]	-		-
OP-715	c.248delC + c.2182_2183delGG	-		-
OP-741	[p.Ala83Valfs82*]+[p.Arg942Met insTrp]			
OP-750	c.2712-1G>T+c.3089T>C; p.Leu1030Pro het.	-		-?
OP-780	exon 3, c.248delC; p.Ala83fs*83 hom.	-	-	-
OP-799	p.Ala83Valfs82* + splicing-mut.	-		-
OP-852	c.248delC + c.2832+4A>G (ex17 donor splice site)	-	-	-
OP-862	exon 3, c.248delC + exon 19 c.3097A>T, p.Lys1033* beide het.	-	-	-
OP-1072 II1	del exon 1 + 2 hom.	-		-
OP-1186	hom., exon 14, c.2440C>T, p.Arg814*	-	-	-
OP- 1261 II1	c.2630delG, p.Glu877Argfs*8 hom.	-		-
OP-1263	GC>G exon 3, c.248delC + exon13, c.2182_2183delGG; p.Gly728Alafs*26 beide het.	-	-	-
OP-1475 II1	c.1345C>T, p.Arg449* + c.3175C>T; p.Arg1059*	-		-
OP-1753 II1	c.248delC (hom.) Dänemark	-		-

2.1.2 Immunofluorescence Staining

Respiratory epithelial cells obtained by nasal brush biopsy were suspended in cell culture medium (RPMI). Samples were spread onto glass slides, air dried and stored at −80°C until use. For the IF staining, cells were incubated in 1x PBS for 5 min to remove cell culture media. Cells were fixed with 4% PFA for 15 minutes at room temperature, washed 2x with 1xPBS and then permeabilized with 0.2% TritonX100 for 10 minutes. After 3 more washes with 1xPBS cells were incubated with 1% skim milk in 1xPBS over night at 4°C or in 2.5% skim milk in 1xPBS for 3 hours at room temperature. The cells were then incubated with primary antibodies for 4 hours at room temperature or overnight at 4°C using the following dilutions: anti-DNAH1 1:50 (rabbit polyclonal; Atlas Antibodies); anti-DNAH6 1:400 (rabbit polyclonal; Atlas Antibodies); anti-DNAH7 1:100 (rabbit polyclonal; Sigma) and anti-acetylated alpha tubulin 1:10000 (mouse monoclonal; Sigma) (Table 5).

After primary antibody incubation, cells were washed 5x with 1x PBS. Cells were incubated with secondary anti-rabbit antibody (goat polyclonal conjugated with Alexa Fluor® 546 fluorophore; Molecular Probes Invitrogen) and secondary anti-mouse antibody (goat polyclonal conjugated with Alexa Fluor® 488 fluorophore; Molecular Probes Invitrogen) diluted 1:1000 each in 1% or 2.5% skim milk in 1xPBS (Table 6). DNA was stained using Hoechst 33342 (1:1000 dilution, Sigma-Aldrich). Cells were finally washed 5X with 1xPBS, mounted in DAKO® Faramount Fluorescent Mounting Medium. High-resolution fluorescence images were taken with a Zeiss AxioObserver.Z1 microscope equipped with an Apotome (Carl Zeiss Microscopy GmbH, Jena, GER). The images were processed with AxioVision 4.8.2 (Carl Zeiss Microscopy GmbH, Jena, GER) and Adobe Creative Suite CS4 (Adobe systems, San José, USA) [44] (Table 7-11).

Materials and Methods

2.2 Materials

2.2.1 Primary Antibodies

Table 5: Primary Antibodies

Antibody	HPA-#	Organism	Dilution IF	Blocking solution and time	Incubation time	Company
polyclonal anti-DNAH1	036805	Rabbit	1:50	5% milk 3 h RT	4°C o/n	Atlas Antibodies (Stockholm, SWE)
polyclonal anti-DNAH6	036391	Rabbit	1:400	1% milk o/n 4°C	3-4 h RT	Atlas Antibodies (Stockholm, SWE)
polyclonal anti-DNAH7	034724	Rabbit	1:100	1% milk o/n 4°C	3-4 h RT	Sigma Prestige Antib. (St. Louis, USA)
monoclonal anti-acetylated α-tubulin	-	Mouse	1:10000	dependent on the other primary antibody		Sigma-Aldrich Co. LLC (St. Louis, USA)

2.2.2 Secondary Antibodies and Nuclei Staining

Table 6: Secondary Antibodies and Nuclei Staining

Product	Company (city, country)
Goat anti-Rabbit IgG (H+L) Secondary Antibody, Alexa Fluor® 546 conjugate	Invitrogen Life Technologies (Carlsbad, USA)
Goat anti-Mouse IgG (H+L) Secondary Antibody, Alexa Fluor® 488 conjugate	Invitrogen Life Technologies (Carlsbad, USA)
bisBenzimide H 33342 trihydrochloride for fluorescence, ≥97.0% (HPLC)	Sigma-Aldrich Co. LLC (St. Louis, USA

2.2.3 Chemicals

Table 7: Chemicals

Chemicals	Company (city, country)
DAKO® Fluorescent Mounting Medium	Dako North America, Inc. (Carpinteria, USA)
Immersol™ 518F	Carl Zeiss Jena GmbH (Oberkochen, GER)

Milchpulver Blotting Grade, pulv., fettarm	CARL ROTH GMBH + CO. KG (Karlsruhe, GER)
Paraformaldehyde, reagent grade, crystalline	Sigma-Aldrich Co. LLC (St. Louis, USA)
PBS Phosphate-Buffered Saline (10X) pH 7.4	Life Technologies (Carlsbad, USA)
Triton-X-100, T8787-100ML	Sigma-Aldrich Co. LLC (St. Louis, USA)

2.2.4 Ingredients of used solutions

Table 8: Ingredients of used solutions

Solutions	
4% PFA	4 g PFA dissolved in 100 ml 1x PBS (60°C), add a few drops of NaOH, adjust pH to 7.4
0.2% Triton X	100 µl Triton X-100 in 50 ml PBS
1% (5%) skim milk solution	0.5 mg (2.5 mg) skim milk powder mixed with 50 ml PBS

2.2.5 Software and Programs

Table 9: Software and Programs

Software/Program	Company (city, country)
Adobe Creative Suite CS4	Adobe Systems (San José, USA)
AxioVision 4.8.2	Carl Zeiss Microscopy GmbH (Jena, GER)

2.2.6 Consumable Materials

Table 10: Consumable Materials

Material	Company (city, country)
BoilProof Mikrozentrifugengefäße 2 ml	Kisker Biotech GmbH & Co KG (Steinfurt, GER)
Cytobrush® Plus GT	Cooper Surgical (Trumbull, USA)

Deckgläser für Mikroskopie 24x50mm no.1	Engelbrecht Medizin und Labortechnik GmbH (Edermünde, GER)
Eppendorf Tubes® 5.0 mL Eppendorf Quality™	Eppendorf AG (Hamburg, GER)
Labmarker Securliner MarkerII/SUPERFROST®	Aspen Surgical (Caledonia, USA)
Leukosilk®	BSN medical GmbH (Hamburg, GER)
Pasteur Pipette glas	Brand GmbH + CO KG (Wertheim, GER)
Permanent Marker Schneider Maxx 220s	Schneider Schreibgeräte GmbH (Schramberg, GER)
Pipette Tips 0,1-1000µl (blue, yellow, grey)	Sarstedt AG & Co. (Nümbrecht, GER)
Reagiergefäß 1.5 ml SafeSeal	Sarstedt AG & Co. (Nümbrecht, GER)
Super PAP Pen Liquid Blocker	Science Services GmbH (München, GER)
Tork Wash Cloth folded	SCA Hygiene Products (Gothenborg, SWE)
Wischtücher clean and clever	IGEFA Handelsgesellschaft mbH & Co. KG (Ahrensfelde, GER)

2.2.7 Laboratory Equipment

Table 11: Laboratory Equipment

Equipment	Productname	Company (city, country)
Zeiss Apotome microscope	Zeiss AxioObserver.Z1 microscope equipped with Apotome	(Carl Zeiss Microscopy GmbH, Jena, GER)
Freezer (-20 °C)	-	Liebherr-International Deutschland GmbH (Biberach, GER)
Freezer (-80 °C)	-86°C Laboratory Freezer	EWALD Innovationstechnik GmbH (Bad Nenndorf, GER)
Millipore System	Milli-Q Integral Wasseraufbereitungssystem	Merck KGaA (Darmstadt, GER)
Pipetboy	pipetus®	Hirschmann Laborgeräte GmbH & Co. KG (Eberstadt, GER)
		Brand GmbH + CO KG (Wertheim, GER)

Materials and Methods

Pipettes	Transferpipette® S, Variabel (D2,5/D10/D20/D100/D200/D1000)	Eppendorf AG (Hamburg, GER)
	Eppendorf Research® plus 0,1-2,5/1-10/2-20/20-200/100-1000/1000-5000 µl	
	Eppendorf Reference® 0,1-2,5/0,5-10 µl	
Refrigerator	-	Liebherr-International Deutschland GmbH (Biberach, GER)
Rotator	Tube rotator	VWR International GmbH (Erlangen, GER)
Timer	'Triple Time' Digitaler 3-fachTimer	TFA Dostmann GmbH & Co. KG (Wertheim, GER)
Vortexer	Vortex Genie2	Scientific Industries (New York, USA)

3   Results

Mutations in *CCDC39* and *CCDC40* cause defects of IDA subgroup I2

The *Chlamydomonas* orthologue of the human DNAH1 is DHC2, which represents one of the heavy chains in the IDA group I2. Western blot analyses (performed by Inga M. Höben) using an anti-DNAH1 antibody detected a specific band at about 490 kDa, which resembles the predicted molecular size of 493.9 kDa of the IDA heavy chain DNAH1. In high-resolution IF analyses on healthy subjects the co-staining of DNAH1 with the cilia marker acetylated tubulin showed a localization of DNAH1 along the entire length of ciliary axonemes (Figure 5 A). I next analyzed by high-resolution IF the distribution of DNAH1 in human respiratory cilia from 7 PCD individuals with mutations in *CCDC39* and 24 PCD individuals with mutations in *CCDC40* (Table 3 and Table 4). In contrast to ciliary axonemes of healthy controls, DNAH1 was completely absent from the ciliary axonemes in every individual analyzed carrying a mutation either in *CCDC39* or in *CCDC40* (Figure 5 B and C). DNAH1 is one of three distinct heavy chains associated with the IDA light chain DNALI1 and these findings are consistent with published results shown by Merveille et al. and Becker-Heck et al. [4, 36], where DNALI1 is also absent from CCDC39 and CCDC40 deficient axonemes.

Mutations in *CCDC39* and *CCDC40* cause defects of IDA subgroup I3

The human orthologue of the heavy chain DHC7 of IDA subgroup I3 is DNAH6. Western Blot analyses (performed by Inga M. Höben) using human spheroids axonemal extract and an antibody directed against DNAH6 detected one specific band at about 480 kDa consistent with the predicted molecular size of DNAH6 (476 kDa). Human respiratory cilia from 3 PCD individuals with mutations in *CCDC39*, from 9 PCD individuals with mutations in *CCDC40* and from healthy donors were then co-stained with antibodies directed against DNAH6 and acetylated tubulin as a control marker. In cilia from healthy donors DNAH6 was observed throughout the respiratory ciliary axoneme (Figure 6 A), indicating that assembled IDAs contain these heavy chains along the entire length of

the ciliary axoneme. In individuals carrying a mutation either in *CCDC39* or in *CCDC40* (Figure 6 B and C), DNAH6 was absent from the ciliary axoneme. These findings show that defects of the 96 nm axonemal ruler caused by mutations in *CCDC39* and *CCDC40* affect also the single-headed IDAs from subgroup I3.

The human orthologue of *Chlamydomonas* heavy chain DHC5, belonging to the IDA group I3, is DNAH7. Immunoblotting analyses (performed by Inga M. Höben) of human axonemal extract using an antibody directed against DNAH7 revealed one single specific band at approximately 465 kDa, which matches the predicted size of DNAH7 (461,2 kDa). I used this antibody to confirm the results generated with the anti-DNAH6 antibody. Therefore, I analyzed cilia from 8 PCD individuals with mutations in *CCDC39*, from 22 PCD individuals with mutations in *CCDC40* and from healthy donors by high-resolution immunofluorescence microscopy. In cilia from healthy donors DNAH7 was observed throughout the respiratory ciliary axoneme (Figure 7 A), indicating that assembled IDAs contain these heavy chains along the entire length of the ciliary axoneme. However, individuals carrying mutations either in *CCDC39* or in *CCDC40*, showed absence of DNAH7 from the ciliary axoneme (Figure 7 B and C). These findings support my previous results with the anti-DNAH6 antibody and support the conclusion, that not only DNALI1-associated IDAs are affected in human respiratory cilia with mutations in *CCDC39* and *CCDC40*, but also centrin-associated IDAs.

Isolated N-DRC-defects and defects of the ODAs do not affect the assembly and axonemal localization of IDAs

I could also show that the absence of single-headed IDAs is characteristic for defects of the 96 nm axonemal ruler. Interestingly, neither isolated nexin-dynein regulatory complex defects caused by mutations in *CCDC164*, *CCDC65* and *GAS8* nor defects of the ODAs lead to any IDA abnormalities (Figure 8-10). I analyzed cilia from PCD individual OP-1627II1 with mutations in *GAS8*, from PCD individual OP-59II1 with mutations in *CCDC164*, from PCD individual OP-835II5 with mutations in *CCDC65*, from PCD individual OP-80II4 with mutations in *DNAH5* and from healthy donors by high-resolution immunofluorescence mi-

croscopy with antibodies directed against DNAH1, DNAH6, DNAH7 and acety-lated tubulin. The three heavy chains of distinct single-headed IDAs and the ciliary control marker were detected along the entire ciliary axoneme of all above-mentioned samples (Table 12).

Table 12: Summary of IF-results for PCD individuals with mutations in genes encoding components of the nexin-dynein regulatory complex or the outer dynein arm complex

PCD ind.	Mutation	DNAH1	DNAH6	DNAH7
OP-1627 II1	*GAS8*: c.1069C<T, p.Gln357* hom.	+	+	+
OP-59 II1	*CCDC164*: c.C352T (p.Gln118*) hom.	+	+	+
OP-835 II5	*CCDC65*: (exon 6) c.877_878delAT; p.Ile293Profs*1	+	+	+
OP-80 II4	*DNAH5*: Ex.63 c.10815delT p.Pro3606His fs22* het.	+	+	+
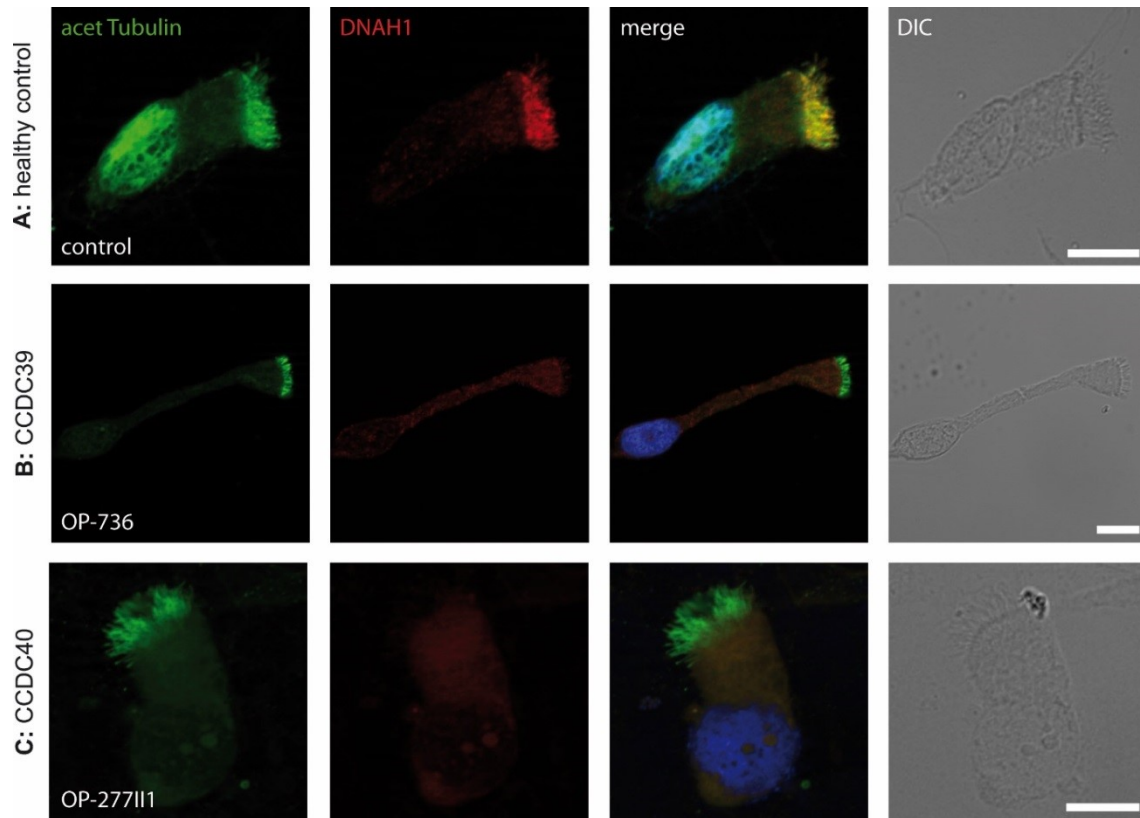
Figure 5: Localization of the IDA axonemal heavy chain DNAH1 in respiratory cells from controls and PCD individuals with mutations in *CCDC39* and *CCDC40*.

A: Representative immunofluorescent images of control respiratory cells show localization of DNAH1 (red) along the entire length of the ciliary axonemes. **B**: Complete absence of DNAH1 from axonemes from patient OP-736 carrying *CCDC39* mutations ([p.Glu851*]+splicing-mutation). **C**: Complete absence of DNAH1 from axonemes from patient OP-277II1 carrying mutations in *CCDC40* ([p.Arg942MetinsTrp]+[p.Gln1043fs36*]). **A –C**: Anti-acetylated alpha tubulin (green) was used to stain the axonemes. Nuclei were stained using Hoechst33342 (blue). The yellow staining (**A**) shows co-localization of DNAH1 and acetylated alpha tubulin in healthy controls. DIC indicates differential interference contrast microscopy images. Scale bars represent 10µm.
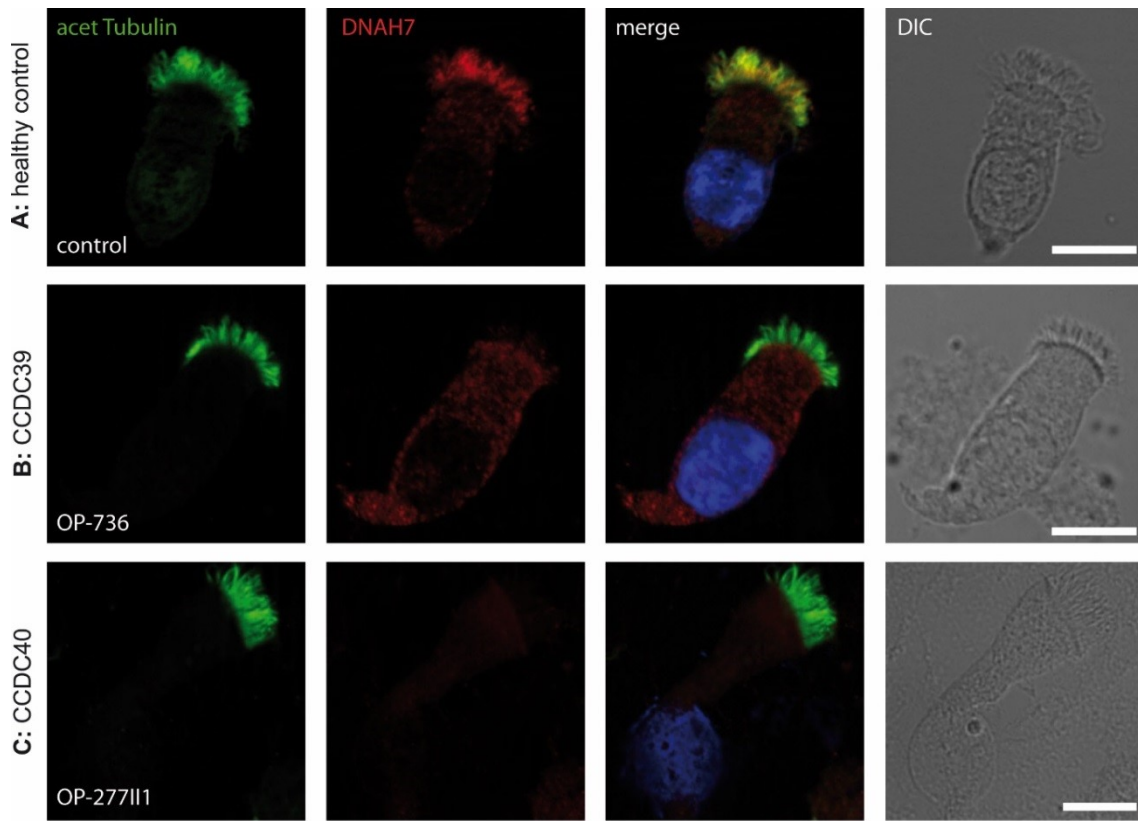
Figure 6: Localization of the IDA axonemal heavy chain DNAH6 in respiratory cells from controls and PCD individuals with mutations in *CCDC39* and *CCDC40*.

A: Representative immunofluorescent images of control respiratory cells show localization of DNAH6 (red) along the entire length of the ciliary axonemes **B**: Complete absence of DNAH6 from axonemes from patient OP-336II1 carrying *CCDC39* mutations (ex. 9: c.1036-2A>C hom). **C**: Complete absence of DNAH6 from axonemes from patient OP-277II1 carrying mutations in *CCDC40* ([p.Arg942MetinsTrp]+[p.Gln1043fs36*]). **A –C**: Anti-acetylated alpha tubulin (green) was used to stain the axonemes. Nuclei were stained using Hoechst33342 (blue). The yellow staining (**A**) shows co-localization of DNAH6 and acetylated alpha tubulin in healthy controls. DIC indicates differential interference contrast microscopy images. Scale bars represent 10µm.

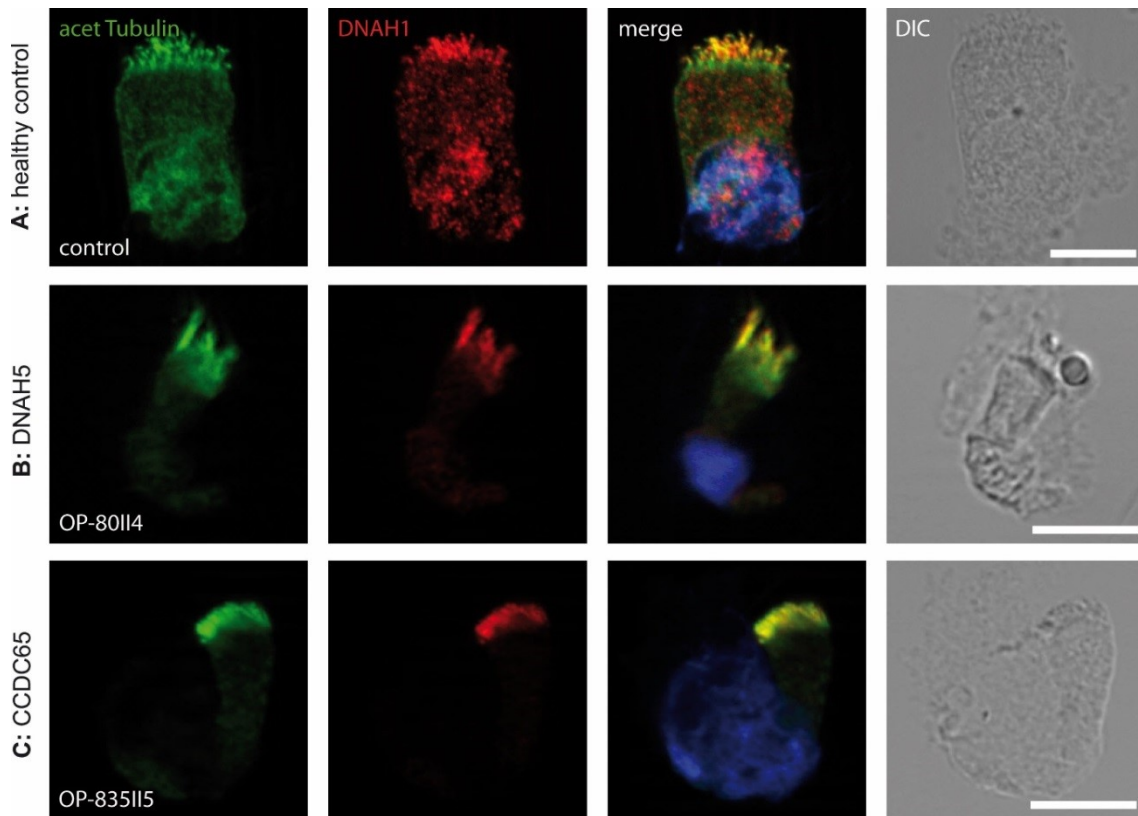**Figure 7:** Localization of the IDA axonemal heavy chain DNAH7 in respiratory cilia from controls and PCD individuals with mutations in *CCDC39* and *CCDC40*.

A: Representative immunofluorescent images of control respiratory cells show localization of DNAH7 (red) along the entire length of the ciliary axonemes **B**: Complete absence of DNAH7 from axonemes from patient OP-736 carrying *CCDC39* mutations ([p.Glu851*]+splicing-mutation). **C**: Complete absence of DNAH7 from axonemes from patient OP-277II1 carrying *CCDC40* mutations ([p.Arg942MetinsTrp]+[p.Gln1043fs36*]). **A-C**: Anti-acetylated alpha tubulin (green) was used to stain the axonemes. Nuclei were stained using Hoechst33342 (blue). The yellow staining (**A**) shows co-localization of DNAH7 and acetylated alpha tubulin in healthy controls. DIC indicates differential interference contrast microscopy images. Scale bar represent 10µm.
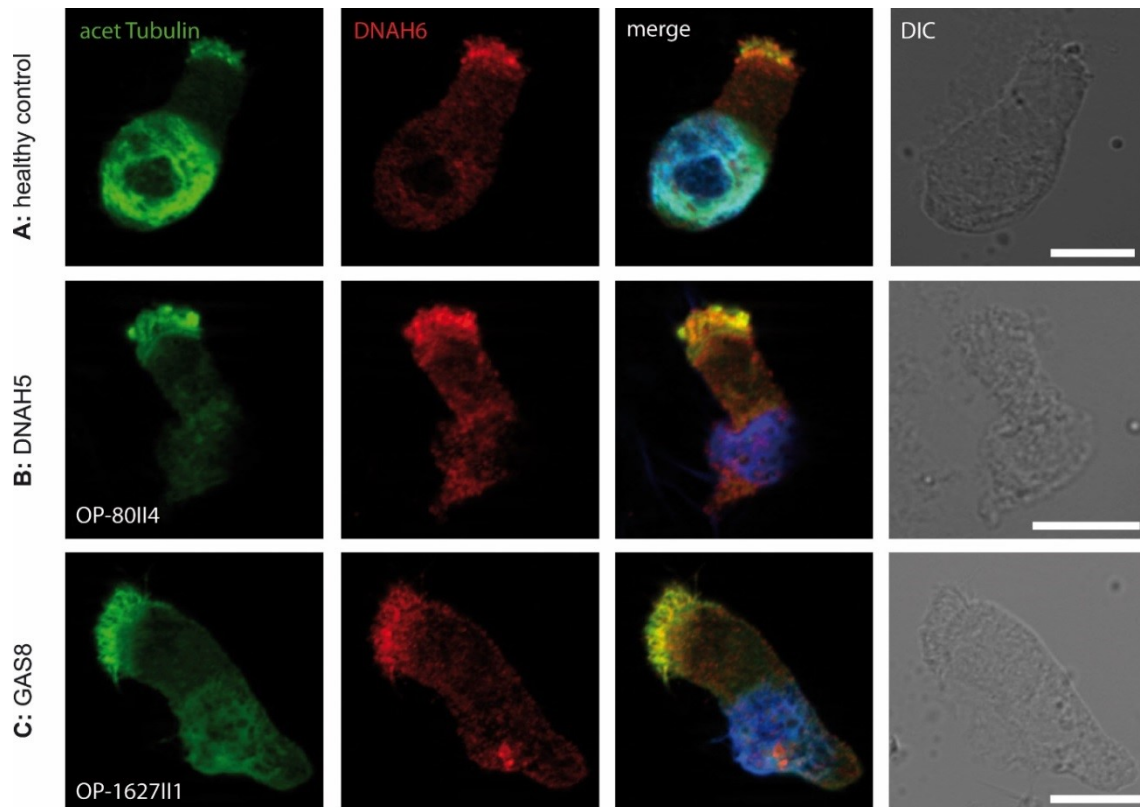
Figure 8: Localization of axonemal DNAH1 in respiratory cells from controls and PCD individuals with mutations in *DNAH5* and *CCDC65.*

A: Representative immunofluorescent images of control respiratory cells show localization of DNAH1 (red) along the entire length of the ciliary axonemes. **B+C**: In respiratory cells from PCD individual OP-80II4 carrying mutations in *DNAH5* (ex.63: c.10815delT; p.Pro3606Hisfs22* het.) (**B**) and from PCD individual OP-835II5 carrying mutations in *CCDC65* (ex.6: c.877_878delAT; p.Ile293Profs*1) (**C**) DNAH1 also localizes along the entire ciliary axoneme. **A-C**: Anti-acetylated alpha tubulin (green) was used to stain the axonemes. Nuclei were stained using Hoechst33342 (blue). The yellow staining shows co-localization of DNAH1 and acetylated alpha tubulin. DIC indicates differential interference contrast microscopy images. Scale bars represent 10µm.

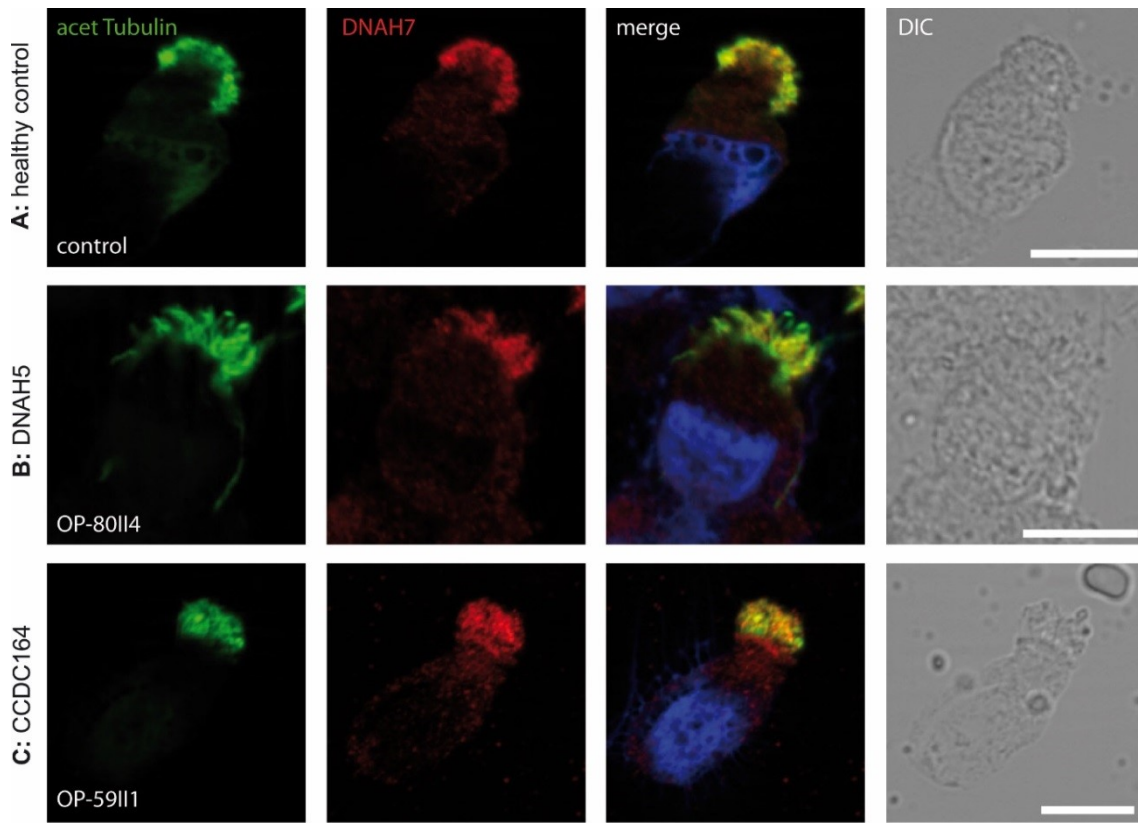**Figure 9:** Localization of axonemal DNAH6 in respiratory cells from controls and PCD individuals with mutations in *DNAH5* and *GAS8.*

A: Representative immunofluorescent images of control respiratory cells show localization of DNAH6 (red) along the entire length of the ciliary axonemes. **B+C**: In respiratory cells from patient OP-80II4 carrying mutations in *DNAH5* (ex.63: c.10815delT; p.Pro3606Hisfs22* het.) (**B**) and from patient OP-1627II1 carrying mutations in *GAS8* (c.1069C<T; p.Gln357* hom.) (**C**) DNAH6 also localizes along the entire ciliary axoneme. **A-C**: Anti-acetylated alpha tubulin (green) was used to stain the axonemes. Nuclei were stained using Hoechst33342 (blue). The yellow staining shows co-localization of DNAH6 and acetylated alpha tubulin. DIC indicates differential interference contrast microscopy images. Scale bars represent 10µm.

Figure 10: Localization of axonemal DNAH7 in respiratory cells from controls and PCD individuals with mutations in *DNAH5* and *CCDC164.*

A: Representative immunofluorescent images of control respiratory cells show localization of DNAH7 (red) along the entire length of the ciliary axonemes. **B+C**: In respiratory cells from patient OP-80II4 carrying mutations in *DNAH5* (ex.63: c.10815delT; p.Pro3606Hisfs22* het.) (**B**) and from patient OP-59II1 carrying mutations in *CCDC164* (c.C352T (p.Gln118*) hom.) (**C**) DNAH7 also localizes along the entire ciliary axoneme. **A-C**: Anti-acetylated alpha tubulin (green) was used to stain the axonemes. Nuclei were stained using Hoechst33342 (blue). The yellow staining shows co-localization of DNAH7 and acetylated alpha tubulin. DIC indicates differential interference contrast microscopy images. Scale bars represent 10μm.

4   Discussion

The aim of this study was to characterize the IDA defects in human respiratory cilia with mutations in *CCDC39* and *CCDC40* in more detail using antibodies directed against different IDA heavy chains. Until now, IDA defects in PCD individuals were characterized by high-resolution IF microscopy using an antibody directed against the IDA light chain DNALI1 (human orthologue to p28) [4, 36], which classifies only the IDA subgroup I2. In *Chlamydomonas,* IDAs are divided into the double-headed IDA I1 and single-headed IDAs. The single-headed IDAs are all associated with the intermediate chain actin and either the light chain p28 or centrin (Table 2) [31, 53, 66]. Based on these findings the single-headed IDAs are further classified into the p28-associated subgroup I2 and the centrin-associated subgroup I3 (Figure 4). In order to investigate on these two subgroups of single-headed dyneins, I used commercially available antibodies directed against the human IDA heavy chains (HCs) DNAH1, DNAH6 and DNAH7, which are orthologous to the *Chlamydomonas* IDA-HCs DHC2, DHC7 and DHC3 (Table 2).

By showing the absence of DNAH1 in human respiratory cilia with mutations in *CCDC39* and *CCDC40* I confirmed alterations in IDAs of subgroup I2. These findings are consistent with the absence of DNALI1 from the ciliary axonemes of *CCDC39* and *CCDC40* mutants [4, 36]. In future diagnostics the antibody anti-DNAH1 might be used to confirm results achieved with the antibody anti-DNALI1.

Furthermore, I showed the absence of DNAH6 and DNAH7 in human respiratory cilia with mutations in *CCDC39* and *CCDC40.* These IDA-HCs are associated with centrin and represent IDAs from the subgroup I3.

It is the first time that also subgroup I3 and in consequence both subgroups, which define every single-headed IDA, were systematically analyzed. The complete lack of every single-headed IDA, which I examined in this study, is supporting the idea of Oda et al [40], that CCDC39 and CCDC40 provide anchoring

Discussion

sites for inner dynein arms. By using these antibodies directed against IDA heavy chains, we now have additional tools to further characterize IDA composition in order to improve PCD diagnostics. In future analysis the involvement of the double-headed IDA remains to be investigated.

Furthermore, by demonstrating a normal IDA distribution in other relevant nexin-link and ODA defects (*CCDC65, CCDC164, GAS8* and *DNAH5*) I illustrated that structural abnormalities of single-headed IDAs are characteristic for defects in *CCDC39* and *CCDC40* (Table 12).

Taken together, my findings support strong evidence for the important role of CCDC39 and CCDC40 in the IDA arrangement of human respiratory cilia. The so called 96 nm axonemal ruler is not only crucial to determine the ciliary 96 nm repeat length of IDAs [40], but also to organize their localization within the axoneme. Moreover, I believe that the classification of IDAs, as it is used in *Chlamydomonas reinhardtii*, is also very useful in the characterization of human IDAs. This model organism is still of great importance for a better understanding of cilia-related disorders.

The results of this work will help to understand the biology of the 96 nm axonemal ruler and its function in humans, taking into account the detailed sub-classification of IDAs as we find it in human respiratory cilia. Research on the 96 nm axonemal ruler is crucial, considering that PCD individuals with biallelic mutations in *CCDC39* and *CCDC40* or associated ultrastructural defects show a very severe clinical presentation of PCD [10].

5 Summary

Motile cilia and flagella show a unique ultrastructure, which is characterized by a central microtubule pair and nine peripheral microtubule doublets. Several protein complexes such as outer and inner dynein arms, radial spokes, the central pair and the nexin-dynein regulatory complex are crucial for ciliary beating pattern and beat frequency. Primary Ciliary Dyskinesia (PCD) is a genetically heterogeneous, autosomal-recessive disorder caused by defects of motile cilia, which result in disturbed mucociliary clearance of the airways and lead to severe respiratory symptoms among others. Therefore, early diagnosis and a better understanding of this disease are essential for an adequate treatment without delay. Different methods are applied for PCD diagnostics including transmission electron microscopy (TEM), high speed video microscopy (HVMA), the measurement of the nasal nitric oxide (nNO) production rate and high resolution immunofluorescence analyses (IF).

The aim of my work was to characterize the defects of the IDA subgroups I2 and I3 in human respiratory cilia with mutations in *CCDC39* and *CCDC40*, which cause defects of the 96 nm axonemal ruler. Mutations in *CCDC39* and *CCDC40* are responsible for at least 12% of all PCD cases [9, 48, 58] and lead to a very severe clinical phenotype [10]. CCDC39 and CCDC40 deficient cilia show tubular disorganization in TEM [1] and a stiff and uncoordinated beating pattern in HVMA [4, 9, 36].

IDAs can be classified in one double-headed IDA I1 and in six single-headed IDAs, which are further divided in subgroups I2 and I3, depending on their association with DNALI1 (p28) or centrin. The absence of the N-DRC and IDAs in *CCDC39* and *CCDC40* mutants was already shown, using IF techniques and antibodies directed against GAS8 (N-DRC) and DNALI1 (IDA) [4, 36]. Nevertheless, the antibody anti-DNALI1 can only confirm the absence of IDAs of the subgroup I2. Until now, IDAs of subgroup I3 have not been examined in human cilia with mutations in *CCDC39* and *CCDC40*. I used IF techniques with the antibodies anti-DNAH1, anti-DNAH6 and anti-DNAH7 to characterize the defect of

Summary

the different IDA subgroups in cilia with mutations in *CCDC39* and *CCDC40*. By showing the absence of DNAH1 in human respiratory cilia with mutations in *CCDC39* and *CCDC40*, I confirmed the absence of IDAs of subgroup I2, which was until now only possible with the antibody anti-DNALI1. In the next step, I showed the absence of IDAs from subgroup I3 in *CCDC39* and *CCDC40* mutants by using the antibodies anti-DNAH6 and anti-DNAH7. It is the first time that both subgroups I2 and I3 were systematically analyzed in human respiratory cilia with mutations in *CCDC39* and *CCDC40*.

I could show that these new antibodies are valuable tools, which will improve PCD diagnostics. Although additional ultrastructural and subcellular localization data are still necessary, the results of this work will help to obtain a more detailed comprehension of the 96 nm axonemal ruler and its function in humans.

6   References

1. Antony D, Becker-Heck A, Zariwala M A et al. (2013) Mutations in CCDC39 and CCDC40 are the major cause of primary ciliary dyskinesia with axonemal disorganization and absent inner dynein arms. Human mutation 34: 462–472.

2. Bartoloni L, Blouin J-L, Pan Y et al. (2002) Mutations in the DNAH11 (axonemal heavy chain dynein type 11) gene cause one form of situs inversus totalis and most likely primary ciliary dyskinesia. Proceedings of the National Academy of Sciences of the United States of America 99: 10282–10286.

3. Becker-Heck A, Loges N T, Omran H (2012) Dynein dysfunction as a cause of primary ciliary dyskinesia and other ciliopathies: 602–627.

4. Becker-Heck A, Zohn I E, Okabe N et al. (2011) The coiled-coil domain containing protein CCDC40 is essential for motile cilia function and left-right axis formation. Nature genetics 43: 79–84.

5. Ben Khelifa M, Coutton C, Zouari R et al. (2014) Mutations in DNAH1, which encodes an inner arm heavy chain dynein, lead to male infertility from multiple morphological abnormalities of the sperm flagella. American journal of human genetics 94: 95–104.

6. Bui K H, Sakakibara H, Movassagh T et al. (2008) Molecular architecture of inner dynein arms in situ in Chlamydomonas reinhardtii flagella. The Journal of cell biology 183: 923–932.

7. Bui K H, Yagi T, Yamamoto R et al. (2012) Polarity and asymmetry in the arrangement of dynein and related structures in the Chlamydomonas axoneme. The Journal of cell biology 198: 913–925.

8. Castleman V H, Romio L, Chodhari R et al. (2009) Mutations in radial spoke head protein genes RSPH9 and RSPH4A cause primary ciliary dyskinesia with central-microtubular-pair abnormalities. American journal of human genetics 84: 197–209.

References

9. Chilvers M (2003) Ciliary beat pattern is associated with specific ultrastructural defects in primary ciliary dyskinesia. Journal of Allergy and Clinical Immunology 112: 518–524.

10. Davis S D, Ferkol T W, Rosenfeld M et al. (2015) Clinical features of childhood primary ciliary dyskinesia by genotype and ultrastructural phenotype. American journal of respiratory and critical care medicine 191: 316–324.

11. DiBella L M (2004) The LC7 light chains of chlamydomonas flagellar dyneins interact with components required for both motor assembly and regulation. Molecular Biology of the Cell 15: 4633–4646.

12. DiBella L M, Smith E F, Patel-King R S et al. (2004) A novel Tctex2-related light chain is required for stability of inner dynein arm I1 and motor function in the Chlamydomonas flagellum. The Journal of biological chemistry 279: 21666–21676.

13. Duquesnoy P, Escudier E, Vincensini L et al. (2009) Loss-of-function mutations in the human ortholog of Chlamydomonas reinhardtii ODA7 disrupt dynein arm assembly and cause primary ciliary dyskinesia. American journal of human genetics 85: 890–896.

14. Duriez B, Duquesnoy P, Escudier E et al. (2007) A common variant in combination with a nonsense mutation in a member of the thioredoxin family causes primary ciliary dyskinesia. Proceedings of the National Academy of Sciences of the United States of America 104: 3336–3341.

15. Fliegauf M, Benzing T, Omran H (2007) When cilia go bad: cilia defects and ciliopathies. Nature reviews. Molecular cell biology 8: 880–893.

16. Goodenough U W, Heuser J E (1985) Substructure of inner dynein arms, radial spokes, and the central pair/projection complex of cilia and flagella. The Journal of cell biology 100: 2008–2018.

17. Harrison A, Olds-Clarke P, King S M (1998) Identification of the t complex-encoded cytoplasmic dynein light chain tctex1 in inner arm I1 supports the involvement of flagellar dyneins in meiotic drive. The Journal of cell biology 140: 1137–1147.

References

18. Hendrickson T W, Perrone C A, Griffin P et al. (2004) IC138 is a WD-repeat dynein intermediate chain required for light chain assembly and regulation of flagellar bending. Molecular Biology of the Cell 15: 5431–5442.

19. Heuser T, Barber C F, Lin J et al. (2012) Cryoelectron tomography reveals doublet-specific structures and unique interactions in the I1 dynein. Proceedings of the National Academy of Sciences 109: E2067-E2076.

20. Heuser T, Raytchev M, Krell J et al. (2009) The dynein regulatory complex is the nexin link and a major regulatory node in cilia and flagella. The Journal of cell biology 187: 921–933.

21. Hjeij R, Onoufriadis A, Watson C M et al. (2014) CCDC151 mutations cause primary ciliary dyskinesia by disruption of the outer dynein arm docking complex formation. American journal of human genetics 95: 257–274.

22. Horani A, Druley T E, Zariwala M A et al. (2012) Whole-exome capture and sequencing identifies HEATR2 mutation as a cause of primary ciliary dyskinesia. American journal of human genetics 91: 685–693.

23. Ikeda K, Yamamoto R, Wirschell M et al. (2009) A novel ankyrin-repeat protein interacts with the regulatory proteins of inner arm dynein f (I1) of Chlamydomonas reinhardtii. Cell motility and the cytoskeleton 66: 448–456.

24. Imtiaz F, Allam R, Ramzan K et al. (2015) Variation in DNAH1 may contribute to primary ciliary dyskinesia. BMC medical genetics 16: 14.

25. Kamiya R, Yagi T (2014) Functional diversity of axonemal dyneins as assessed by in vitro and in vivo motility assays of Chlamydomonas mutants. Zoological science 31: 633–644.

26. King S M, Kamiya R (2009) Axonemal Dyneins: 131–208.

27. Knowles M R, Leigh M W, Carson J L et al. (2012a) Mutations of DNAH11 in patients with primary ciliary dyskinesia with normal ciliary ultrastructure. Thorax 67: 433–441.

References

28. Knowles M R, Leigh M W, Ostrowski L E et al. (2012b) Exome sequencing identifies mutations in CCDC114 as a cause of primary ciliary dyskinesia. American journal of human genetics 92: 99–106.

29. Konrádová V, Vavrová V, Hlousková Z et al. (1982) Ultrastructure of bronchial epithelium in children with chronic or recurrent respiratory diseases. European journal of respiratory diseases 63: 516–525.

30. Kott E, Duquesnoy P, Copin B et al. (2012) Loss-of-function mutations in LRRC6, a gene essential for proper axonemal assembly of inner and outer dynein arms, cause primary ciliary dyskinesia. American journal of human genetics 91: 958–964.

31. LeDizet M, Piperno G (1995) The light chain p28 associates with a subset of inner dynein arm heavy chains in Chlamydomonas axonemes. Molecular Biology of the Cell 6: 697–711.

32. Loges N T, Olbrich H, Becker-Heck A et al. (2009) Deletions and point mutations of LRRC50 cause primary ciliary dyskinesia due to dynein arm defects. American journal of human genetics 85: 883–889.

33. Loges N T, Olbrich H, Fenske L et al. (2008) DNAI2 mutations cause primary ciliary dyskinesia with defects in the outer dynein arm. American journal of human genetics 83: 547–558.

34. Mastronarde D N, O'Toole E T, McDonald K L et al. (1992) Arrangement of inner dynein arms in wild-type and mutant flagella of Chlamydomonas. The Journal of cell biology 118: 1145–1162.

35. Mazor M, Alkrinawi S, Chalifa-Caspi V et al. (2011) Primary ciliary dyskinesia caused by homozygous mutation in DNAL1, encoding dynein light chain 1. American journal of human genetics 88: 599–607.

36. Merveille A-C, Davis E E, Becker-Heck A et al. (2011) CCDC39 is required for assembly of inner dynein arms and the dynein regulatory complex and for normal ciliary motility in humans and dogs. Nature genetics 43: 72–78.

References

37. Mitchison H M, Schmidts M, Loges N T et al. (2012) Mutations in axonemal dynein assembly factor DNAAF3 cause primary ciliary dyskinesia. Nature genetics 44: 381-9, 1-2.

38. Myster S H, Knott J A, O'Toole E et al. (1997) The Chlamydomonas Dhc1 gene encodes a dynein heavy chain subunit required for assembly of the I1 inner arm complex. Molecular Biology of the Cell 8: 607–620.

39. Myster S H, Knott J A, Wysocki K M et al. (1999) Domains in the 1alpha dynein heavy chain required for inner arm assembly and flagellar motility in Chlamydomonas. The Journal of cell biology 146: 801–818.

40. Oda T, Yanagisawa H, Kamiya R et al. (2014) A molecular ruler determines the repeat length in eukaryotic cilia and flagella. Science (New York, N.Y.) 346: 857–860.

41. Olbrich H, Häffner K, Kispert A et al. (2002) Mutations in DNAH5 cause primary ciliary dyskinesia and randomization of left-right asymmetry. Nature genetics 30: 143–144.

42. Olbrich H, Schmidts M, Werner C et al. (2012) Recessive HYDIN mutations cause primary ciliary dyskinesia without randomization of left-right body asymmetry. American journal of human genetics 91: 672–684.

43. Omran H, Kobayashi D, Olbrich H et al. (2008) Ktu/PF13 is required for cytoplasmic pre-assembly of axonemal dyneins. Nature 456: 611–616.

44. Omran H, Loges N T (2009) Immunofluorescence staining of ciliated respiratory epithelial cells 91: 123–133.

45. Onoufriadis A, Paff T, Antony D et al. (2012) Splice-site mutations in the axonemal outer dynein arm docking complex gene CCDC114 cause primary ciliary dyskinesia. American journal of human genetics 92: 88–98.

46. Onoufriadis A, Shoemark A, Munye M M et al. (2014) Combined exome and whole-genome sequencing identifies mutations in ARMC4 as a cause of primary ciliary dyskinesia with defects in the outer dynein arm. Journal of medical genetics 51: 61–67.

References

47. Panizzi J R, Becker-Heck A, Castleman V H et al. (2012) CCDC103 mutations cause primary ciliary dyskinesia by disrupting assembly of ciliary dynein arms. Nature genetics 44: 714–719.

48. Papon J F, Coste A, Roudot-Thoraval F et al. (2010) A 20-year experience of electron microscopy in the diagnosis of primary ciliary dyskinesia. The European respiratory journal 35: 1057–1063.

49. Pazour G J (2004) Comparative genomics: prediction of the ciliary and basal body proteome. Current biology : CB 14: R575-7.

50. Pennarun G, Escudier E, Chapelin C et al. (1999) Loss-of-function mutations in a human gene related to Chlamydomonas reinhardtii dynein IC78 result in primary ciliary dyskinesia. American journal of human genetics 65: 1508–1519.

51. Perrone C A, Myster S H, Bower R et al. (2000) Insights into the structural organization of the I1 inner arm dynein from a domain analysis of the 1beta dynein heavy chain. Molecular Biology of the Cell 11: 2297–2313.

52. Perrone C A, Yang P, O'Toole E et al. (1998) The Chlamydomonas IDA7 locus encodes a 140-kDa dynein intermediate chain required to assemble the I1 inner arm complex. Molecular Biology of the Cell 9: 3351–3365.

53. Piperno G (1992) The inner dynein arms I2 interact with a "dynein regulatory complex" in Chlamydomonas flagella. The Journal of cell biology 118: 1455–1463.

54. Piperno G, Ramanis Z, Smith E F et al. (1990) Three distinct inner dynein arms in Chlamydomonas flagella: molecular composition and location in the axoneme. The Journal of cell biology 110: 379–389.

55. Porter M E (1992) Extragenic suppressors of paralyzed flagellar mutations in Chlamydomonas reinhardtii identify loci that alter the inner dynein arms. The Journal of cell biology 118: 1163–1176.

56. Porter M E, Sale W S (2000) The 9 + 2 axoneme anchors multiple inner arm dyneins and a network of kinases and phosphatases that control motility. The Journal of cell biology 151: F37-F42.

References

57. Schneeberger E E, McCormack J, Issenberg H J et al. (1980) Heterogeneity of ciliary morphology in the immotile-cilia syndrome in man. Journal of ultrastructure research 73: 34–43.

58. Shoemark A, Dixon M, Corrin B et al. (2012) Twenty-year review of quantitative transmission electron microscopy for the diagnosis of primary ciliary dyskinesia. Journal of clinical pathology 65: 267–271.

59. Smith E F, Sale W S (1991) Microtubule binding and translocation by inner dynein arm subtype I1. Cell motility and the cytoskeleton 18: 258–268.

60. Springer A L, Bruhn D F, Kinzel K W et al. (2011) Silencing of a putative inner arm dynein heavy chain results in flagellar immotility in Trypanosoma brucei. Molecular and biochemical parasitology 175: 68–75.

61. Toba S, Fox L A, Sakakibara H et al. (2011) Distinct roles of 1alpha and 1beta heavy chains of the inner arm dynein I1 of Chlamydomonas flagella. Molecular Biology of the Cell 22: 342–353.

62. Wallmeier J, Shiratori H, Dougherty G W et al. (2016) TTC25 deficiency results in defects of the outer dynein arm docking machinery and primary ciliary dyskinesia with left-right body asymmetry randomization. American journal of human genetics 99: 460–469.

63. Wirschell M, Olbrich H, Werner C et al. (2013) The nexin-dynein regulatory complex subunit DRC1 is essential for motile cilia function in algae and humans. Nature genetics 45: 262–268.

64. Wirschell M, Yang C, Yang P et al. (2009) IC97 is a novel intermediate chain of I1 dynein that interacts with tubulin and regulates interdoublet sliding. Molecular Biology of the Cell 20: 3044–3054.

65. Yagi T, Uematsu K, Liu Z et al. (2009) Identification of dyneins that localize exclusively to the proximal portion of Chlamydomonas flagella. Journal of cell science 122: 1306–1314.

66. Yanagisawa H, Kamiya R (2001) Association between actin and light chains in Chlamydomonas flagellar inner-arm dyneins. Biochemical and Biophysical Research Communications 288: 443–447.

7   List of figures

8   List of tables

9   Acknowledgements

10 Curriculum Vitae

11 Votum of the ethics committee

ÄRZTEKAMMER
WESTFALEN-LIPPE

medizinische
fakultät

ETHIK
KOMMISSION
der Ärztekammer Westfalen-Lippe
und der Medizinischen Fakultät der
Westfälischen Wilhelms-Universität

Gartenstraße 210 – 214
48147 Münster, Germany
Tel.: +49 (0)251 929 2460
Fax: +49 (0)251 929 2478
E-Mail: ethik-kommission@aekwl.de
www.ethik-kommission.uni-muenster.de

Ethik-Kommission Münster · Gartenstraße 210 – 214 · 48147 Münster

Herrn
Univ.-Prof. Dr. med. Heymut Omran
Klinik für Kinder- und Jugendmedizin -
Allgemeine Pädiatrie -
Universitätsklinikum Münster
Albert-Schweitzer-Campus 1, Gebäude A1
48149 Münster

2. März 2015

Unser Aktenzeichen: **2015-104-f-S** (bitte immer angeben!)
Studiencode: (PCD)
Sponsor / Finanzierung: Universitätsklinikum Münser, Klinik für Kinder- und Jugendmedizin,
Allgemeine Pädiatrie, Univ.-Prof. Dr. med. Heymut Omran, Albert-Schweitzer-Campus 1, Gebaude
A1, 48149 Münster
Titel des Forschungsvorhabens:
„Charakterisierung der Erkrankungsbilder des Flimmerepithels inklusive der Primären Zilitären
Dyskinesie"

Votum

Sehr geehrter Herr Professor Omran,

für das oben genannte Forschungsvorhaben haben Sie mit Schreiben vom 27.01.2015 die Beratung
durch die Ethik-Kommission der Ärztekammer Westfalen-Lippe und der Medizinischen Fakultät der
Westfälischen Wilhelms-Universität Münster („Ethik-Kommission") beantragt.

Nachdem die im Vorfeld entstandenen Unstimmigkeiten am 26.01.2015 in der Geschäftsstelle der
Ethik-Kommission mit Ihnen vorgesprochen worden sind, hat die Ethik-Kommission in ihrer Sitzung
am 30.01.2015 über Ihren Antrag beraten, die von Ihnen ergänzend eingereichten Unterlagen in
einem Ausschuss geprüft und beschlossen:

**Die Ethik-Kommission hat keine grundsätzlichen Bedenken ethischer oder rechtlicher Art
gegen die Durchführung des Forschungsvorhabens.**

Die Ethik-Kommission erteilt jedoch die folgenden Hinweise:

Bitte reichen Sie noch die in der Patientenaufklärung für Eltern (S. 3) erwähnte Liste der Mitarbeiter
Ihrer Klinik, die Zugriff auf die Liste mit den Nummerncodes haben, nach.

Die vorliegende Einschätzung gilt für das Forschungsvorhaben, wie es sich auf Grundlage der in
Anhang 1 genannten Unterlagen darstellt.

Für die Entscheidung der Ethik-Kommission erhebt die Ärztekammer Westfalen-Lippe Gebühren
nach Maßgabe ihrer Verwaltungsgebührenordnung. Über die auf 20 / 50 % der Regelgebühr
ermäßigten Gebühren erhalten Sie von der Ärztekammer einen gesonderten Bescheid.

Mitglieder: H. W. Bothe (Vorsitzender), H. Pfeiffer (stellv. Vorsitzende),
F. U. Müller, P. Scheutzel, R. Rapp-Engels, M. Fücking, P. Huxkonbroch, J. Ritter, G. Rudolf, H.-D. Steinmeyer, D. Voß, W. Engemann

Votum of the ethics committee

Allgemeine Hinweise:

Die Einschätzung der Kommission ist als ergebnisoffene Beratung für den Antragsteller nicht bindend. Die Ethik-Kommission weist darauf hin, dass unabhängig von der vorliegenden Stellungnahme die medizinische, ethische und rechtliche Verantwortung für die Durchführung des Forschungsvorhabens bei dessen Leiter und bei allen an dem Vorhaben teilnehmenden Ärzten bzw. Forschern verbleibt.

An der Beratung und Beschlussfassung haben die in Anhang 2 aufgeführten Mitglieder der Ethik-Kommission teilgenommen. Es haben keine Kommissionsmitglieder teilgenommen, die selbst an dem Forschungsvorhaben mitwirken oder deren Interessen davon berührt werden.

Die Ethik-Kommission empfiehlt im Einklang mit der Deklaration von Helsinki *nachdrücklich die* Registrierung klinischer Studien vor Studienbeginn in einem öffentlich zugänglichen Register, das die von der Weltgesundheitsorganisation (WHO) geforderten Voraussetzungen erfüllt, insbesondere deren Mindestangaben enthält. Ausführliche Informationen zur International Clinical Trials Registry Platform (ICTRP) stehen im Internetangebot der WHO zur Verfügung:
http://www.who.int/ictrp/about/en/
Zu den Kriterien des International Committee of Medical Journal Editors (ICMJE) sei beispielsweise verwiesen auf die Informationen unter:
http://www.icmje.org/recommendations/browse/publishing-and-editorial-issues/clinical-trial-registration.html
Das WHO Primär-Register für Deutschland ist das Deutsche Register für Klinische Studien (DRKS) in Freiburg. Es erfüllt die Forderungen der Fachzeitschriften:
http://www.drks.de/index.html

Die Ethik-Kommission der Ärztekammer Westfalen-Lippe und der Medizinischen Fakultät der Westfälischen Wilhelms-Universität Münster ist organisiert und arbeitet gemäß den nationalen gesetzlichen Bestimmungen und den GCP-Richtlinien der ICH.

Die Kommission wünscht Ihrem Forschungsvorhaben gutes Gelingen und geht davon aus, dass Sie nach Abschluss des Vorhabens über die Ergebnisse berichten werden.

Mit freundlichen Grüßen

Univ.-Prof. Dr. med. Hans-Werner Bothe M.A.
Vorsitzender der Ethik-Kommission

Votum of the ethics committee

Anhang 1

Folgende Unterlagen haben bei der Beschlussfassung vorgelegen:

Eingang	Datierung	Anlage
28.01.2015	27.01.2015	Anschreiben Ethik-Kommission 20150127
28.01.2015	27.01.2015	CV_ H. Omran_20150126
28.01.2015	27.01.2015	Ethikantrag_ Flimmerepithel_PCD_20150126
28.01.2015	27.01.2015	Fragen zum Ethik-Antrag 2014-588-f-S_DFG-IZKF_20150123
28.01.2015	27.01.2015	P Flimmerepithel_Kind Jugendlicher_Version01_27012015
28.01.2015	27.01.2015	P+E Flimmerepithel_Erziehungsberechtigte_Version01_27012015
28.01.2015	27.01.2015	P+E Flimmerepithel_Patient_Version01_27012015
28.01.2015	27.01.2015	Studienprotokoll_Flimmerepithel_PCD__20150126
19.01.2015	18.01.2015	P Flimmerepithel_Kind Jugendlicher_Version02_13022015
19.01.2015	18.01.2015	P Flimmerepithel_Kind Jugendlicher_Version02_13022015_track changes
19.01.2015	18.01.2015	P+E Flimmerepithel_Erziehungsberechtigte_Version02_13022015
19.01.2015	18.01.2015	P+E Flimmerepithel_Erziehungsberechtigte_Version02_13022015_track changes
19.01.2015	18.01.2015	P+E Flimmerepithel_Patient_Version02_13022015
19.01.2015	18.01.2015	P+E Flimmerepithel_Patient_Version02_13022015_track changes

Votum of the ethics committee

Anhang 2

Folgende Mitglieder der Ethik-Kommission haben an der Beratung und Beschlussfassung in der Sitzung vom 30.01.2015 teilgenommen:

Univ.-Prof. Dr. med. Hans-Werner **Bothe** M.A.
Klinik für Neurochirurgie
Universitätsklinikum Münster
Vorsitzender

Univ.-Prof. em. Dr. med. Jörg **Ritter**
Klinik für Kinder- und Jugendmedizin
- Pädiatrische Hämatologie und Onkologie -
Universitätsklinikum Münster

Univ.-Prof. Dr. med. Frank U. **Müller**
Institut für Pharmakologie und Toxikologie
Universitätsklinikum Münster

Prof. Dr. med. Heinrich **Schulze Mönking**
St. Rochus-Hospital Telgte
Fachklinik für Psychiatrie und Psychotherapie

Frau Dr. rer. nat. Dorothea **Voß**
Apotheke des UKM
Universitätsklinikum Münster

Frau Dr. med. Regine **Rapp-Engels**
Fachärztin für Allgemeinmedizin
- Sozialmedizin -
Münster

Frau Mechthild **Föcking**
Landesarbeitsgemeinschaft der Selbsthilfe Behinderter e.V.
Münster

Herr Klaus **Schelp**
Präsident des Landgerichts
Landgericht Münster

Frau Univ.-Prof. Dr. med. Heidi **Pfeiffer**
Institut für Rechtsmedizin
Universitätsklinikum Münster

-

S. 4 von 4